SRTTU

JCARME
ISSN: 2228-7922

Journal of Computational and Applied Research
in Mechanical Engineering
Vol. 3, No. 2, pp. 145-159, Spring 2014
http://jcarme.srttu.edu

Nonlinear static and dynamic behaviors of a microresonator under discontinuous electrostatic actuation

M. Zamanian* **and S. A. A. Hosseini**

Faculty of Engineering, Kharazmi University, Mofatteh Avenue, P.O. Box 15719-14911, Tehran, Iran

Article info:
Received: 02/07/2013
Accepted: 30/11/2013
Online: 03/03/2014

Keywords:
Microbeam,
Electrostatic actuation,
Natural frequency,
Nonlinear vibration,
Galerkin method,
Perturbation method.

Abstract
This article studied static deflection, natural frequency and nonlinear vibration of a clamped-clamped microbeam under discontinues electrostatic actuation. The electrostatic actuation was induced by applying AC-DC voltage between the microbeam and electrode plate. In contrast to previous works, it was assumed that length of the electrode plate was smaller than that of the microbeam. In addition, it was assumed that a layer whose length was equal to that of the electrode plate was deposited on the lower side of the microbeam. Equation of motion was derived using Newton's second law. The static deflection due to the DC electrostatic actuation and the natural frequency about this position were obtained using the Galerkin method. Nonlinear vibration of the system due to the AC electrostatic actuation was obtained using the multiple scale perturbation method. Variations of static deflection, pull-in voltage, natural frequency and frequency response of vibration about the static deflection of microbeam with respect to variations of second layer length, second layer thickness, electrode plate length and value of electrostatic actuation were also studied. It was shown that, depending on the value of these parameters, static deflection and natural frequency of vibration about static deflection increased or decreased. Moreover, it was demonstrated that, depending on the value of these system parameters, nonlinear vibration of the system due to the AC electrostatic actuation might be realized as a softening or hardening behavior.

1. Introduction

Electrostatically actuated microbeam is a major component of many of resonant sensors. Electrostatic actuation is induced by applying an AC-DC voltage between the microbeam and an electrode plate which is on the opposite side of the microbeam. The DC component deflects the microbeam to a new equilibrium position (static deflection) while the AC component vibrates the microbeam around this equilibrium position [1].

Many works have been performed to analyze mechanical behavior of microresonator

*Corresponding author
Email address: zamanian@khu.ac.ir

systems. These works might be categorized in two main groups. In the first group, nonlinear effect of electrostatic actuation, mid-plane stretching and nonlinear curvature on static and dynamic behaviors of a clamped-clamped or clamped-free microbeam have been studied. In the second group, effect of changing geometry of microbeam or ground electrode shape on the mechanical behavior of system has been discovered.

The important works in the first category may be as follows: Tilmans and Legtenberg used the Rayleigh-Ritz method to obtain natural frequency and static deflection of microbeam, where midplane stretching was neglected [2]. Chio and Lovell obtained static deflection by numerical shooting method and considering the stiffening midplane stretching term [3]. Abdel-Rahman et al. studied effect of DC electrostatic actuation on the value of pull-in voltage and natural frequency of vibration about static deflection using numerical shooting method [4]. They considered nonlinear terms of stretching and electrostatic actuation. Younis et al. performed the previous work using the Galerkin method [5]. The static deflection and dynamic behavior of clamped-free microresonators under DC electrostatic actuation or combined AC-DC electrostatic actuation have been studied in [6-10]. Younis and Nayfeh [1], Abdel-Rahman and Nayfeh [11] have investigated primary and secondary resonances of clamped-clamped microresonator, respectively, considered nonlinear effect of AC-DC electrostatic and stretching terms and solved equation of motion using multiple scale perturbation method. Jia et al. considered the forced vibration of clamped-clamped electrically actuated microbeam near resonance frequency by considering the intermolecular force [12].

The important works in the second category may be as follows: Najar et al. analyzed static deflection and motion of a shaped microbeam using differential quadrature method (DQM) [13] and showed that an increase (decrease) in the gap size between midsection of microbeam and electrode plate in comparison with gap size of the end sections resulted in an increase (decrease) in the pull-in voltage. Abdalla et al. considered optimizing shape of an electrostatic actuated microbeam for maximum pull-in voltage [14]. Nie et al. [15] and Rezazadeh [16] studied pull-in voltage of multilayered microbeam and solved the equation of motion using finite difference method. Wang et al. investigated pull-in instability and vibrational behaviors for a multi-layer microbeam using shooting method [17]. Jia et al. studied pull-in instability and free vibration of microbeam with an emphasis on the effect of ground electrode shape [18]. Sadeghian et al. studied pull-in voltage of a clamped-clamped microbeam under discontinuous electrostatic actuation by letting length of electrode plate be smaller than that of the microbeam [19]. They demonstrated that variation in the electrostatic area caused variation in pull-in voltage. A similar result was reported by Younis for a clamped-clamped microbeam by assuming that two parts of the microbeam length were covered by electrode [20].

The literature shows that previously performed works on the microbeam including partially electrostatic actuation have focused on static deflection and pull-in voltage of systems. They have not studied their natural frequency and forced vibration. So, the first novelty in this paper was in investigating the natural frequency and forced vibration of microbeam under discontinuous (partially) electrostatic actuation.

The second novelty was that thickness of the microbeam in the part under electrostatic actuation was assumed to be two layered. This assumption caused deflection shape of the microbeam in that part to be more uniform than the part that was single layer, which was due to the increase of the moment of inertia in the cross section of the microbeam. This phenomenon is very useful in designing microsensor system. For example, in a pressure sensor, pressure change could cause the microbeam to deflect to a new position; so, electric capacity of the system would changed. Change of capacity induces an electric current. It is a criterion for calculating the amount of changing pressure. The more uniform the deflection shape of microbeam, the more linear the signal would be, which would be very useful [21]. So, in this paper, static and

dynamic behaviors of this configuration were studied for the first time.

In this study, first, the static deflection due to the DC electrostatic actuation and the natural frequency about this position were obtained using the Galerkin method. Then, nonlinear vibration of the system due to the AC electrostatic actuation at primary resonance was obtained using the multiple scale perturbation method.

2. Modeling and formulation

The system model was a two layered clamped-clamped microbeam. A thin layer of the electrode was deposited on the lower side of the second layer and there was an electrode plate at distance d from this layer. An AC-DC voltage equal to $v_p + v_{ac}\cos(\hat{\Omega}t)$ was applied between them. In this actuation, v_{ac} and $\hat{\Omega}$ are amplitude and frequency of the AC part, respectively. Also, v_p is magnitude of DC part and t is time. It was assumed that the left and right ends of electrode plate were at distances l_1 and l_2 from the left end of the microbeam. Length of lower layer was assumed to be equal to the length of electrode plate Fig. 1(a). It was assumed that one end of the microbeam was stretched equal to $\bar{\varepsilon}$ in the axial direction due to the existence of axial load. It must be noted that the microbeam was not free to deflect in axial direction, but its right end was maintained to remain in the constant position which was obtained by applying the axial load. Two coordinate systems were used to describe the equations of motion. The first coordinate system was a fixed Cartezian coordinate system, syz, the origin of which was located at the left end of the microbeam on the neutral axis of the system cross section Fig. 1(b). The second coordinate system was the local coordinate system, $\bar{s}\bar{y}\bar{z}$, the origin of which was located on the neutral axis of the deflected system cross section. It was assumed that the microbeam was initially displaced by U and W with respect to the fixed coordinate system. The motion equations for a beam subjected to a transverse load per unit length, q_2, might be written as follows [22, 23]:

(1)

$$(F_1\cos(\theta))' + (\frac{M_3'\sin(\theta)}{1+e})' = m(s)\ddot{U},$$

$$(F_1\sin(\theta))' - (\frac{M_3'\cos(\theta)}{1+e})' + q_2 = m(s)\ddot{W},$$

$$U(0,t) = 0,\ U(l,t) = \bar{\varepsilon},$$

$$W(0,t) = 0,\ W(l,t) = 0,\ \frac{\partial W(0,t)}{\partial s} = 0,\ \frac{\partial W(l,t)}{\partial s} = 0$$

where e is stretching strain of the neutral axis of cross section, M_3 is bending moment and F_1 is equivalent axial force in the cross section of deflected microbeam, as shown in Fig. 1(b). In addition, the dot and prime signs show differentiation with respect to s and t, respectively.

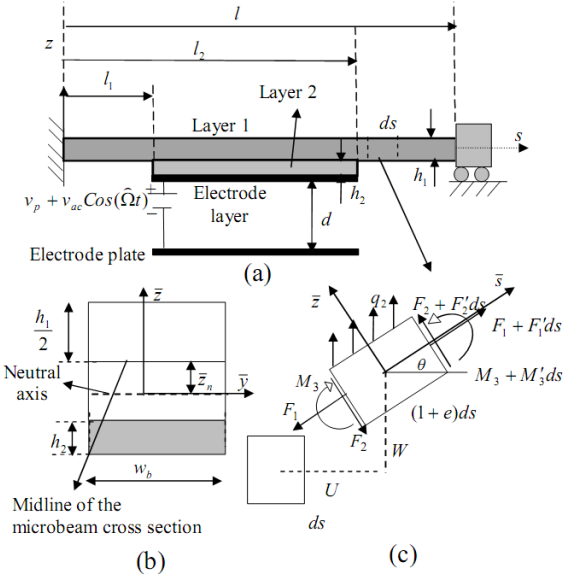

Fig. 1. (a) System model, (b) the system cross section when $l_1 \le s \le l_2$, and (c) free body diagrams of a deflected element.

Here, q_2 is sum of load per unit length of microbeam due to the electrostatic field and air damping, which may be written as follows [1]:

$$q_2 = -\hat{c}\dot{W} - \frac{(H_{l_1} - H_{l_2})0.5\varepsilon_0 w_b (v_p + v_{ac}\cos(\hat{\Omega}t))^2}{(d+W)^2} \qquad (2)$$

where $H_{l_i}, i=1,2$ means the Heaviside function; i.e. it is equal to zero for $s<l_i$ and is equal to one for $s\geq l_i$. Also, $\hat{c}$ is viscous damping per unit length of microbeam and ε_0 is dielectric permittivity in vacuum. The expression of $m(s)$ is mass per unit length of the microbeam; so:

$$m(s)=w_b(\rho_1 h_1+(H_{l_1}-H_{l_2})\rho_2 h_2) \tag{3}$$

where $h_1(h_2)$ and $\rho_1(\rho_2)$ are thickness and mass per unit volume of the first and second layers of microbeam, respectively. It must be noted that the second layer referred to the lower layer of microbeam. In addition, w_b is width of the first and second layers of the microbeam. It should be notified that thickness effect of the electrode layer was neglected because of being very thin. The relationship between stress and strain for the first and second layers might be constructed as follows:

$$\sigma_1=E_1\varepsilon_1, \quad \sigma_2=E_2\varepsilon_2 \tag{4}$$

where σ_1 (ε_1) and σ_2 (ε_2) are stress (strain) in the axial direction of local coordinate system for the first and second layers, respectively. Also, E_1 and E_2 are elasticity modulus of the first and second layers, respectively. The strain in the cross section of the microbeam might be written as follows [22, 23]:

$$\varepsilon_i = e-\kappa\bar{z}, \qquad i=1,\ 2 \tag{5}$$

where κ is curvature of the deflected microbeam in the sz plane. The second layer was not attached to the entire length of the microbeam. So, in the section in which there was no second layer, the neutral axis was the midline of the first layer cross section; and on the section in which the second layer was attached, the neutral axis was at distance $\bar{z}_n$ from the midline of microbeam cross section, as shown in Fig. 1(c), which can be written as follows [23]:

$$\bar{z}_n = \frac{E_2 h_2 (h_2+h_1)}{2(E_1 h_1+E_2 h_2)} \tag{6}$$

Now, by considering Eq. (4), the axial load and bending moment in the cross section of the system might be written as follows:

$$\begin{aligned} F_1 &= \int \sigma_1 dA_1+(H_{l_1}-H_{l_2})\int \sigma_2 dA_2 =(1-H_{l_1})\times \\ &\int_{-h_1/2}^{h_1/2} E_1\varepsilon_1 w_b d\bar{z}+(H_{l_1}-H_{l_2})\int_{-h_1/2+\bar{z}_n}^{h_1/2+\bar{z}_n} E_1\varepsilon_1 w_b d\bar{z}+ \\ &(H_{l_1}-H_{l_2})\int_{-h_2-h_1/2+\bar{z}_n}^{-h_1/2+\bar{z}_n} E_2\varepsilon_2 w_b d\bar{z}+ \\ &H_{l_2}\int_{-h_1/2}^{h_1/2} E_1\varepsilon_1 w_b d\bar{z} \end{aligned} \tag{7}$$

and

$$\begin{aligned} M_3 &= -\int \sigma_1\bar{z}dA_1-(H_{l_1}-H_{l_2})\int \sigma_2\bar{z}dA_2= \\ &-(1-H_{l_1})\int_{-h_1/2}^{h_1/2} E_1\varepsilon_1 w_b\bar{z}d\bar{z}-(H_{l_1}-H_{l_2})\times \\ &\int_{-h_1/2+\bar{z}_n}^{h_1/2+\bar{z}_n} E_1\varepsilon_1 w_b\bar{z}d\bar{z}-(H_{l_1}-H_{l_2})\times \\ &\int_{-h_2-h_1/2+\bar{z}_n}^{-h_1/2+\bar{z}_n} E_2\varepsilon_2 w_b\bar{z}d\bar{z}-H_{l_2}\int_{-h_1/2}^{h_1/2} E_1\varepsilon_1 w_b\bar{z}d\bar{z} \end{aligned} \tag{8}$$

where dA_1 and dA_2 show area differential element of the first and second layers of the microbeam, respectively. It must be noted that midplane stretching, e, curvature, κ, and terms of $\sin(\theta)$ and $\cos(\theta)$ in Eq. (1) could be written in terms of U and W using the Taylor series [22, 23]. So, by substituting Eq. (5) in Eqs. (7) and (8) and then substituting the outcome equations in Eq. (1), the equations of motion in axial and lateral directions would be obtained. By combining the resulted equations, the dimensionless form of motion equation would be as shown below [23].

$$\begin{aligned} &\frac{\partial^2}{\partial x^2}\left(H(x)\frac{\partial^2 w}{\partial x^2}\right)+m(x)\frac{\partial^2 w}{\partial \tau^2}+c\frac{\partial w}{\partial \tau}-(\alpha_1\Gamma(w,w)+ \\ &N)\frac{\partial^2 w}{\partial x^2}=(H_{l_1/l}-H_{l_2/l})\frac{\alpha_2(v_p+v_{ac}\cos(\Omega\tau))^2}{(1-w)^2}, \\ &w\big|_{x=0,1}=0, \quad \frac{\partial w}{\partial x}\bigg|_{|x=0,1}=0, \end{aligned} \tag{9}$$

where

$$\begin{aligned} &w=\frac{-W}{d}, \quad x=\frac{s}{l}, \quad \tau=\frac{t}{T}, \quad T=\sqrt{\frac{\rho_1 h_1 w_b l^4}{E_1 I_1}}, \\ &\Gamma(f_1,f_2)=\int_0^l \frac{\partial f_1}{\partial x}\frac{\partial f_2}{\partial x}dx, \end{aligned} \tag{10}$$

In Eq. (9), the terms including $H(x)$, $m(x)$ and c are terms of bending stiffness, mass inertia

and viscous damping, respectively. These terms are [23]:

$$m(x)=1+\frac{\rho_2 h_2}{\rho_1 h_1}(H_{l_1/l}-H_{l_2/l}),\ \ H(x)=(1-H_{l_1/l})+\frac{\bar{I}_1}{I_1}(H_{l_1/l}-H_{l_2/l})+\frac{E_2 I_2}{E_1 I_1}(H_{l_1/l}-H_{l_2/l})+H_{l_2/l},$$
$$c=\frac{\hat{c}l^4}{E_1 I_1 T},\quad I_1=\frac{1}{12}w_b h_1^3,\quad \bar{I}_1=\frac{1}{12}w_b h_1^3+h_1 w_b \bar{z}_n^2,\qquad (11)$$
$$I_2=w_b[\frac{1}{3}(h_2^3+\frac{3}{2}h_1 h_2^2+\frac{3}{4}h_2 h_2^2)+h_2\bar{z}_n^2-(h_2^2+h_2 h_1)\bar{z}_n]$$

In Eq. (9), the term including N is due to the axial load and the term including α_1 is due to stretching effect. These terms are [23]:

$$N=N_b(\frac{1+\frac{E_2 h_2}{E_1 h_1}}{(1+\frac{E_2 h_2}{E_1 h_1})(1-\frac{l_2-l_1}{l})+\frac{l_2-l_1}{l}}),$$
$$\alpha_1=\alpha_b(\frac{1+\frac{E_2 h_2}{E_1 h_1}}{(1+\frac{E_2 h_2}{E_1 h_1})(1-\frac{l_2-l_1}{l})+\frac{l_2-l_1}{l}}),\qquad (12)$$
$$N_b=\frac{\bar{\varepsilon}\,A_b l}{I_b},\quad \alpha_b=6(\frac{d}{h_1})^2,\quad A_b=h_1 w_b$$

By equating differentiation of displacement with respect to time to zero in Eq. (9), differential equation of the static deflection w_s would be:

$$\frac{\partial^2}{\partial x^2}(H(x)\frac{\partial^2 w_s}{\partial x^2})-(\alpha_1\Gamma(w_s,w_s)+N)\frac{\partial^2 w_s}{\partial x^2}=(H_{l_1/l}-H_{l_2/l})\frac{\alpha_2 v_p^2}{(1-w_s)^2},\ w_s\big|_{x=0,1}=0,\frac{dw_s}{dx}\big|_{x=0,1}=0 \qquad (13)$$

Displacement of the system is the sum of static deflection w_s, and dynamic deflection $u(x,\tau)$, so:

$$w(x,\tau)=u(x,\tau)+w_s \qquad (14)$$

By substituting Eq. (14) in Eq. (9), expanding the electrostatic force about the static position and by using Eq. (13), the terms that represent equilibrium position were eliminated and the following was obtained:

$$\frac{\partial^2}{\partial x^2}(H(x)\frac{\partial^2 u}{\partial x^2})+m(x)\frac{\partial^2 u}{\partial \tau^2}+c\frac{\partial u}{\partial \tau}=(\alpha_1\Gamma(w_s,w_s)+N)\frac{\partial^2 u}{\partial x^2}+2\alpha_1\Gamma(w_s,u)\frac{d^2 w_s}{dx^2}+\alpha_1\Gamma(u,u)\frac{d^2 w_s}{dx^2}+2\alpha_1\Gamma(w_s,u)\frac{\partial^2 u}{\partial x^2}+\alpha_1\Gamma(u,u)\frac{\partial^2 u}{\partial x^2}+\frac{2\alpha_2 v_p^2}{(1-w_s)^3}u+\frac{3\alpha_2 v_p^2}{(1-w_s)^4}u^2+\frac{4\alpha_2 v_p^2}{(1-w_s)^5}u^3+(H_{l_1/l}-H_{l_2/l})\times(\frac{2\alpha_2 v_p v_{ac}\cos(\Omega\tau)}{(1-w_s)^2}+\frac{4\alpha_2 v_p v_{ac}\cos(\Omega\tau)}{(1-w_s)^3}u+\frac{\alpha_2(v_{ac}\cos(\Omega\tau))^2}{(1-w_s)^2})\quad u\big|_{x=0,1}=0,\quad \frac{\partial u}{\partial x}\big|_{x=0,1}=0 \qquad (15)$$

If v_{ac} and c ere equal to zero in Eq. (15) and its linear terms were kept, then the linear equation of free vibration of undamped system about the static position would be as follows:

$$\frac{\partial^2}{\partial x^2}(H(x)\frac{\partial^2 u}{\partial x^2})+m(x)\frac{\partial^2 u}{\partial \tau^2}-(\alpha_1\Gamma(w_s,w_s)+N)\times\frac{\partial^2 u}{\partial x^2}-2\alpha_1\Gamma(w_s,u)\frac{d^2 w_s}{dx^2}-(H_{l_1/l}-H_{l_2/l})\times\frac{2\alpha_2 v_p^2}{(1-w_s)^3}u=0,\quad u\big|_{x=0,1}=0,\quad \frac{\partial u}{\partial x}\big|_{x=0,1}=0 \qquad (16)$$

Here, if the system oscillated about the static position by nth natural frequency, then the system vibration might be assumed as:

$$u=\phi_n(x)e^{i\omega_n\tau} \qquad (17)$$

where $\varphi_n(x)$ is the nth linear mode shapes and ω_n is the nth natural frequency of vibration of deflected microbeam about the static position. By substituting Eq. (17) in the free vibration equation and multiplying it by $e^{-i\omega_n\tau}$, the differential equation governed by linear mode shapes of system would be:

$$\frac{\partial^2}{\partial x^2}(H(x)\frac{\partial^2 \phi_n}{\partial x^2})-(\alpha_1\Gamma(w_s,w_s)+N)\frac{d^2\phi_n}{dx^2}-2\alpha_1\Gamma(w_s,\phi_n)\frac{d^2 w_s}{dx^2}-(H_{l_1/l}-H_{l_2/l})(\frac{2\alpha_2 v_p^2}{(1-w_s)^3}+m(x)\omega_n^2)\phi_n=0,\ \phi_n\big|_{x=0,1}=0,\ \frac{d\phi_n}{dx}\big|_{x=0,1}=0 \qquad (18)$$

3. Free vibration about static deflection

Solution of Eq. (13) might be obtained using the Galerkin method. The mode shapes of

vibration of a straight microbeam without the second layer were used as comparison functions. So, solution of Eq. (13) was assumed as:

$$w_s = \sum_{j=1}^{M} a_{[j]}\phi_{s[j]} \tag{19}$$

where $\varphi_{s[j]}$ is the jth linear symmetric mode shapes of a straight microbeam without second layer and $a_{[j]}, j = 1..M$ are the multipliers that must be obtained using the Glaerkin method. By substituting Eq. (19) in Eq. (13), multiplying the resulting equation by $\varphi_{s[n]}, n = 1, 2, 3..,M$ and then integrating the outcome from $x = 0$ to $x = 1$, M algebraic equations can be obtained as follows:

$$\begin{aligned}
&\sum_{j=1}^{M} a_{[j]}\int_0^1 \varphi_{s[n]}\frac{d^2}{dx^2}(H(x)\frac{d^2\varphi_{s[j]}}{dx^2})dx + \\
&\int_0^1 \sum_{j,k,m=1}^{M} a_{[j]}a_{[k]}a_{[m]}\frac{d^2}{dx^2}(H(x)\frac{d^2\varphi_{s[j]}}{dx^2})\varphi_{s[k]}\varphi_{s[m]}\varphi_{s[n]}\,dx - \\
&2\int_0^1 \sum_{j,k=1}^{M} a_{[j]}a_{[k]}\frac{d^2}{dx^2}(H(x)\frac{d^2\varphi_{s[j]}}{dx^2})\varphi_{s[k]}\varphi_{s[n]}\,dx - \\
&\alpha_1 \sum_{j,k,m=1}^{M} a_{[j]}a_{[k]}a_{[m]}\,\Gamma(\varphi_{s[j]},\varphi_{s[k]})\int_0^1 \frac{d^2\varphi_{s[m]}}{dx^2}\varphi_{s[n]}\,dx - \\
&\alpha_1 \sum_{j,k,m,p,q=1}^{M} a_{[j]}a_{[k]}a_{[m]}a_{[p]}a_{[q]}\,\Gamma(\varphi_{s[j]},\varphi_{s[k]})\times \\
&\int_0^1 \frac{d^2\phi_{s[m]}}{dx^2}\phi_{s[p]}\phi_{s[q]}\phi_{s[n]}\,dx + 2\alpha_1 \times \\
&\sum_{j,k,m,p=1}^{M} a_{[j]}a_{[k]}a_{[m]}a_{[p]}\,\Gamma(\phi_{s[j]},\phi_{s[k]})\int_0^1 \frac{d^2\phi_{s[m]}}{dx^2}\times \\
&\phi_{s[p]}\phi_{s[n]}dx - N\sum_{j=1}^{M}\int_0^1 a_{[j]}\frac{d^2\phi_{s[j]}}{dx^2}\phi_{s[n]}\,dx - \\
&N\int_0^1 \sum_{j,k,m=1}^{M} a_{[j]}a_{[k]}a_{[m]}\frac{d^2\phi_{s[j]}}{dx^2}\phi_{s[k]}\phi_{s[m]}\phi_{s[n]}\,dx + \\
&2N\int_0^1 \sum_{j,k=1}^{M} a_{[j]}a_{[k]}\frac{d^2\phi_{s[j]}}{dx^2}\phi_{s[k]}\phi_{s[n]}\,dx - \\
&\alpha_2 v_p^2\int_{l_1/l}^{l_2/l}\phi_{s[n]}\,dx
\end{aligned} \tag{20}$$

The coefficients $a_{[j]}$ would be obtained by solving the algebraic system of Eq. (20). Then, static deflection could be obtained using Eq. (19). Now, the mode shapes and natural frequency, i.e. solution of Eq. (18), was obtained using the Galerkin method .So, the solution of Eq. (18) was assumed as:

$$\phi = \sum_{j=1}^{M} b_{[j]}\phi_{a[j]} \tag{21}$$

where $b_{[j]}, j = 1..M$ are the unknown coefficients that must be obtained using the Galerkin method. By substituting Eq. (21) in (18), multiplying the result by $\varphi_s[n], n = 1,2,..,M$ and integrating from $x = 0$ *to* $x = 1$, an algebraic system was obtained as:

$$\begin{aligned}
&\int_0^1 \sum_{j=1}^{M} b_{[j]}\,(1-w_s)^3\frac{d^2}{dx^2}(H(x)\frac{d^2\phi_{s[j]}}{dx^2})\phi_{s[n]}\,dx - \\
&\int_0^1 \sum_{j=1}^{M} b_{[j]}(1-w_s)^3(\alpha_1\Gamma(w_s,w_s)+N)\frac{d^2\phi_{s[j]}}{dx^2}\phi_{s[n]}dx \\
&-2\alpha_1\int_0^1 \sum_{i=1}^{M} b_{[j]}\,\Gamma(\phi_{s[j]},w_s)\phi_{s[n]}(1-w_s)^3\frac{d^2w_s}{dx^2}dx \\
&-\omega^2\int_0^1 \sum_{j=1}^{M} b_{[j]}m(x)(1-w_s)^3\phi_{s[j]}\phi_{s[n]}\,dx - \\
&2\alpha_2 v_p{}^2\int_{l_1/l}^{l_2/l} \sum_{j=1}^{M} b_{[j]}\phi_{s[j]}\phi_{s[n]}\,dx = 0
\end{aligned} \tag{22}$$

Eq. (22) has a nonzero solution if the determinant of coefficient $b_{[j]}$ in Eq. (22) is equal to zero. So, by equating the determinant of coefficients to zero, the natural frequency can be obtained.

4. Primary resonances

By considering $T_0 = \tau$, $T_1 = \varepsilon\tau$ and $T_2 = \varepsilon^2\tau$ where ε is small non-dimensional bookkeeping parameter, solution of Eq. (15) might be assumed as [1]:

$$\begin{aligned}
&u(x,\tau,\varepsilon) = \varepsilon u_1(x,T_0,T_1,T_2) + \varepsilon^2 u_2(x,T_0,T_1,T_2) + \\
&\varepsilon^3 u_3(x,T_0,T_1,T_2) + ...
\end{aligned} \tag{23}$$

In order to balance the nonlinear terms with the terms of air damping c and excitation v_{ac}, they were considered order ε^2 and ε^3 terms, respectively. The following equations would be obtained by substituting Eq. (23) in Eq. (15) and equating coefficients of the same power of ε .

order (ε) :

$$L(u_1)=m(x)\frac{\partial^2 u_1}{\partial T_0^2}+\frac{\partial^2}{\partial x^2}(H(x)\frac{\partial^2 u_1}{\partial x^2})-(\alpha_1\Gamma(w_s,w_s)+N)\times \frac{\partial^2 u_1}{\partial x^2}-2\alpha_1\Gamma(w_s,u_1)\frac{d^2 w_s}{dx^2}-(H_{l_1/l}-H_{l_2/l})\frac{2\alpha_2 v_p^{\ 2}}{(1-w_s)^3}u_1=0, \quad u_1\big|_{x=0,1}=0,\ \ \frac{\partial u_1}{\partial x}\big|_{x=0,1}=0 \tag{24}$$

order (ε^2) :

$$L(u_2)=\alpha_1\Gamma(u_1,u_1)\frac{d^2 w_s}{dx^2}+2\alpha_1\Gamma(w_s,u_1)\frac{\partial^2 u_1}{\partial x^2}+(H_{l_1/l}-H_{l_2/l})\frac{3\alpha_2 v_p^2}{(1-w_s)^4}u_1^{\ 2}-2m(x)\frac{\partial^2 u_1}{\partial T_0\partial T_1}, \quad u_2\big|_{x=0,1}=0,\ \ \frac{\partial u_2}{\partial x}\big|_{x=0,1}=0 \tag{25}$$

order (ε^3) :

$$L(u_3)=-2m(x)\frac{\partial^2 u_2}{\partial T_0\partial T_1}-m(x)(\frac{\partial^2 u_2}{\partial T_1^2}+2\frac{\partial^2 u_1}{\partial T_0\partial T_2})-c\frac{\partial u_1}{\partial T_0}+2\alpha_1\Gamma(u_1,u_2)\frac{d^2 w_s}{dx^2}+2\alpha_1\Gamma(w_s,u_2)\frac{\partial^2 u_1}{\partial x^2}+2\alpha_1\Gamma(w_s,u_1)\frac{\partial^2 u_2}{\partial x^2}+\alpha_1\Gamma(u_1,u_1)\frac{\partial^2 u_1}{\partial x^2}+(H_{l_1/l}-H_{l_2/l})\times(\frac{6\alpha_2 v_p^2}{(1-w_s)^4}u_1u_2+\frac{4\alpha_2 v_p^2}{(1-w_s)^5}u_1^{\ 3}+\frac{2\alpha_2 v_p v_{ac}\cos(\Omega T_0)}{(1-w_s)^2}), \quad u_3\big|_{x=0,1}=0,\ \ \frac{\partial u_3}{\partial x}\big|_{x=0,1}=0 \tag{26}$$

Using the normalized mode shapes of the system $(\int_0^1\varphi^2dx=1)$, solution of Eq. (24) would be:

$$u_1=A(T_1,T_2)e^{i\omega T_0}\phi(x)+\bar{A}(T_1,T_2)e^{-i\omega T_0}\phi(x) \tag{27}$$

where $\varphi(x)$ and ω show the first mode shape and first natural frequency of the system, respectively. In addition, $A(T_1,T_2)$ is a complex function, which is obtained by imposing the solvability condition. By substituting Eq. (27) in Eq. (25):

$$L(u_2)=(A^2e^{2i\omega T_0}+2A\bar{A}+\bar{A}^2e^{-2i\omega T_0})h(x)-2m(x)\omega i(\frac{\partial A(T_1,T_2)}{\partial T_1}e^{i\omega T_0}-\frac{\partial\bar{A}(T_1,T_2)}{\partial T_1}e^{-i\omega T_0}) \tag{28}$$

where:

$$h(x)=\alpha_1\Gamma(\phi,\phi)\frac{d^2 w_s}{dx^2}+2\alpha_1\Gamma(w_s,\phi)\frac{d^2\phi}{dx^2}+(H_{l_1/l}-H_{l_2/l})\frac{3\alpha_2 v_p^{\ 2}}{(1-w_s)^4}\phi^2 \tag{29}$$

If A only depended on T_2, then the secular term would not arise in Eq. (28). Using this assumption, the particular solution of Eq. (28) would be as follows:

$$u_2=\psi_1(x)A^2e^{2i\omega T_0}+2\psi_2(x)A\bar{A}+\psi_1(x)\bar{A}^2e^{-2i\omega T_0} \tag{30}$$

where:

$$\frac{d^2}{dx^2}(H(x)\frac{d^2\psi_j}{dx^2})-4m(x)\omega^2\delta_{1j}\psi_j-(\alpha_1\Gamma(w_s,w_s)+N)\frac{d^2\psi_j}{dx^2}-2\alpha_1\Gamma(w_s,\psi_j)\frac{d^2 w_s}{dx^2}-(H_{l_1}-H_{l_2})\frac{2\alpha_2 v_p^2}{(1-w_s)^3}\psi_j=h(x),\ \ j=1,2 \quad \psi_j\big|_{x=0,1}=0,\ \ \frac{d\psi_j}{dx}\big|_{x=0,1}=0 \tag{31}$$

where $\delta_{1j}, j=1,2$ is Kronecker delta function. Solution of Eq. (31) might be obtained using the linear symmetric mode shapes of vibration of the microbeam about the static position as comparison functions in Galerkin method. So, it was assumed that:

$$\psi_j=\sum_{k=1}^{M}c_k\phi_k \tag{32}$$

where φ_k shows the kth linear symmetric mode shape of deflected microbeam about static position and c_k are coefficients that must be obtained using the Galerkin method. In fact, by solving the algebraic system obtained by substituting Eq. (32) in Eq. (31), multiplying the results by $\varphi_n, n=1,2,..,M$ and integrating the results from $x=0$ *to* $x=1$, the following could be obtained:

$$\int_0^1\sum_{k=1}^{M}c_k\frac{d^2}{dx^2}(H(x)\frac{d^2\phi_k}{dx^2})\phi_n dx-4\omega^2\delta_{1j}\int_0^1\sum_{k=1}^{M}c_k m(x)\times\phi_k\phi_n dx-\int_0^1\sum_{k=1}^{M}c_k(\alpha_1\Gamma(w_s,w_s)+N)\frac{d^2\phi_k}{dx^2}\phi_n dx-2\alpha_1\int_0^1\sum_{k=1}^{M}c_k\Gamma(\phi_k,w_s)\phi_n\frac{d^2 w_s}{dx^2}dx-2\alpha_2 v_p^{\ 2}\times\int_{l_1/l}^{l_2/l}\sum_{k=1}^{M}c_k\frac{\phi_k\phi_n}{(1-w_s)^3}dx-\int_0^1 h(x)\phi_n dx=0 \tag{33}$$

where $j=1,2$. Now, substituting u_1 and u_2 from Eqs. (27) and (30) in Eq. (26), introducing fundamental natural frequency by detuning parameter σ as $\Omega=\omega+\varepsilon^2\sigma$ and keeping only the terms that produce secular terms would result in:

$$L(u_3)=[-2m(x)\omega i\frac{dA}{dT_2}\phi(x)-i\omega Ac\phi(x)+\chi(x)A^2\bar{A}+\bar{F}(x)e^{i\sigma T_2}]e^{i\omega T_0}+cc+NST \quad (34)$$

where NST shows all terms, that is not secular and cc denotes complex conjugate terms, and:

$$\bar{F}(x)=(H_{l_1/l}-H_{l_2/l})\frac{\alpha_2 v_p v_{ac}}{(1-w_s)^2}, \quad (35)$$

$$\chi(x)=\chi_q^G+\chi_c^G+\chi_q^E+\chi_c^G$$

where

$$\chi_q^G=(2\alpha_1\Gamma(\psi_1,\phi)+4\alpha_1\Gamma(\psi_2,\phi))\frac{d^2w_s}{dx^2}+(2\alpha_1\frac{d^2\psi_1}{dx^2}+4\alpha_1\frac{d^2\psi_2}{dx^2})\Gamma(w_s,\phi)+(2\alpha_1\Gamma(w_s,\psi_1)+4\alpha_1\Gamma(w_s,\psi_2))\frac{d^2\phi}{dx^2}, \quad (36)$$

$$\chi_c^G(x)=3\alpha_1\Gamma(\phi,\phi)\frac{d^2\phi}{dx^2},$$

$$\chi_q^E=(H_{l_1/l}-H_{l_2/l})\frac{6\alpha_2 v_p^2}{(1-w_s)^4}(2\phi\psi_2+\phi\psi_1),$$

$$\chi_c^E=(H_{l_1/l}-H_{l_2/l})\frac{12\alpha_2 v_p^2}{(1-w_s)^5}\phi^3,$$

The left hand side of Eq. (36) is self adjoint; so, the adjoint solution is like solution of homogenous Eq. (24). The non-homogeneous Eq. (36) has a solution only if the right hand side of Eq. (36) is orthogonal to every solution of the self adjoint homogenous equation; i.e. $\varphi(x)e^{i\omega T_0}$. So, by multiplying the right hand side of Eq. (36) to $\varphi(x)e^{-i\omega T_0}$ and integrating the outcome from $x=0$ to $x=1$, the solvability condition can be obtained as:

$$2i\omega(\bar{m}\frac{dA}{dT_2}+\frac{\mu_1 A}{2})+8SA^2\bar{A}-Fe^{i\sigma T_2}=0 \quad (37)$$

where:

$$\mu_1=\int_0^1 c\phi^2 dx, \quad S_q^G=-\frac{1}{8}\int_0^1\chi_q^G\phi\,dx, \quad (38)$$

$$S_c^G=-\frac{1}{8}\int_0^1\chi_c^G\phi\,dx, \quad S_q^E=-\frac{1}{8}\int_0^1\chi_q^E\phi\,dx,$$

$$S_c^E=-\frac{1}{8}\int_0^1\chi_c^E\phi\,dx, \quad \bar{m}=\int_0^1 m(x)\phi^2 dx,$$

$$F=\int_0^1\bar{F}\phi dx,\ S=S_q^G+S_c^G+S_q^E+S_c^E$$

Now, A is denoted in a polar form with amplitude a and phase β as follows:

$$A=1/2\ a\,e^{i\beta} \quad (39)$$

By substituting Eq. (39) in Eq. (37), separating the real and imaginary parts and assuming that $\gamma=\sigma T_2-\beta$, the results would be:

$$\bar{m}\frac{da}{dT_2}=-\frac{\mu_1}{2}a+\frac{F}{\omega}\sin\gamma=f(a,\gamma),$$
$$\bar{m}\frac{d\gamma}{dT_2}=\sigma\bar{m}-\frac{Sa^2}{\omega}+\frac{F}{a\omega}\cos\gamma=g(a,\gamma) \quad (40)$$

By substituting Eqs. (30) and (27) in Eq. (23) and substituting $\varepsilon=1$, solution of Eq. (37) would be:

$$u(x,t)=a\cos(\Omega\tau-\gamma)\phi(x)+\frac{1}{2}a^2(\psi_2(x)+\cos 2(\Omega\tau-\gamma)\psi_1(x)) \quad (41)$$

By letting da/dT_2 and $d\gamma/dT_2$ be equal to zero in Eq. (40), the equilibrium point (a_0,γ_0) could be obtained as:

$$a_0^2[(\frac{\mu_1}{2})^2+(\sigma\bar{m}-\frac{Sa_0^2}{\omega})^2]=\frac{F^2}{\omega^2} \quad (42)$$

This equation shows that amplitude a_0 is a maximum when the expression inside parenthesis vanishes. So, the results would be:

$$\sigma=Sa_0^2/(\omega\bar{m}), \quad a_0=2F/(\omega\mu_1) \quad (43)$$

Also, by considering $\sigma=\Omega-\varepsilon^2\omega$ and combing it with the obtained results, the nonlinear resonance frequency would be obtained as:

$$\Omega=\omega+\frac{4SF^2}{\omega^3\mu_1^2} \quad (44)$$

5. Results and discussion

In the previous work [20], static deflection and pull-in voltage of a microbeam with configuration shown in Fig. 2(a) were studied. In the considered configuration, the electrostatic actuation was applied at two parts of the

microbeam length and there was no second layer. So, assuming $h_2 = 0$ and that multiplier of Eq. 2 according to Heaviside function was as $(H_{l_1} - H_{l_2}) + (H_{l_1'} - H_{l_2'})$, then the results of this work had to be in agreement with those of [20]. This comparison is shown in Fig. 2(b), which demonstrates excellent agreement.

Also, assuming that $h_2 / h_1 = 0, l_2 - l_1 = l$; i.e the electrostatic actuation was applied to all lengths of the microbeam, then value of S which is a criteria for the shift of resonant frequency had to be equal. This comparison is shown in Fig. 3, which demonstrates excellent agreement.

In the following, effect of increasing or decreasing the electrostatic actuation, electrode plate length, thickness and length of the second layer was studied on the deflection, pull in voltage, natural frequency and frequency response of the microbeam with $\alpha_1 = 3.7, N = 8.7$, respectively.

Effect of the electrode plate length on the value of static deflection and natural frequency is shown in Figs. 4 and 5. According to Fig. 4, with increasing the electrode plate length from 0 to l, maximum deflection of microbeam increased.

It increased because, with increasing the length of electrode plate, the area under electrostatic field increased, which caused the equivalent lateral force to increase; so, the static deflection increased. It can be concluded from Fig. 5 that, when $h_2 / h_1 = 0$; i.e. thickness of the second layer was equal to zero, then with increasing the electrode plate length from 0 to l, natural frequency decreased.

These variations were due to the fact that, considering Eq. (16), the electrostatic actuation had a main softening term as $2\alpha_2 v_p^2 u / (1 - w_s)^3$ multiplied by $(H_{l_1} - H_{l_2})$. With increasing the length of electrode plate, value of this softening term increased because value of $(H_{l_1} - H_{l_2})$ and w_s increased. So, increasing length of the electrode plate would decrease the natural frequency of the system. Also, Fig. 5 demonstrates that, for larger values of h_2 / h_1, value of natural frequency increased by increasing value of $l_2 - l_1$, which was different by its variations when h_2 / h_1 was small. This variation was due to the competition between hardening effect of bending stiffness and softening effect of electrostatic actuation.

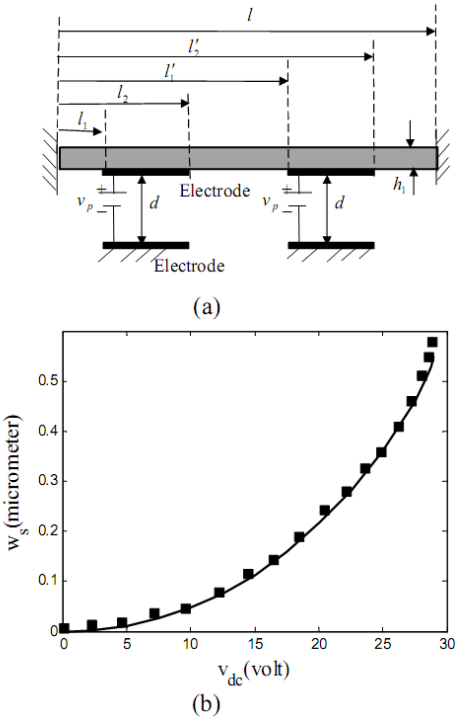

Fig. 2. (a) System model in [20], $l_1 = 0.125l$, $l_2 = 0.375l$, $l_3 = 0.625l, l_4 = 0.875l$, $E_1 = 124GPas$, $l = 100\mu m, h_1 = 0.5\mu m$, $\rho_1 = 2332kg/m^3$, (b) Variations of maximum deflection of microbeam with respect to variations of v_p solid line (this paper), square points [20].

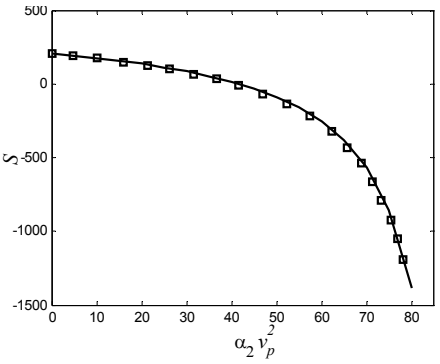

Fig. 3. Variations of nonlinear coefficient S with respect to value of $\alpha_2 v_p^2$; square points belong to [1] and the solid lines belong to this paper $\alpha_1 = 3.7, N = 8.7$.

It is clear that, when $h_2/h_1 \neq 0$, then with increasing value of $l_2 - l_1$, equivalent value of bending stiffness increased. In addition, it caused the main softening term $2\alpha_2 v_p^2 u/(1-w_s)^3$ multiplied by $(H_{l_1} - H_{l_2})$ to increase. For small values of h_2/h_1, with increasing $l_2 - l_1$, increasing effect of bending stiffness was larger than increasing effect of softening electrostatic actuation; and, for larger values of h_2/h_1, this competition was reversed.

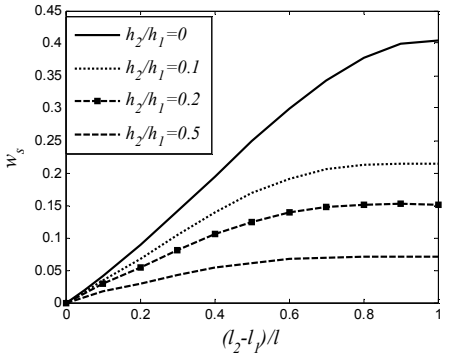

Fig. 4. Maximum deflection variations of the microbeam with respect to the variation of $l_2 - l_1$ for different values of h_2/h_1, where $\alpha_2 v_p^2 = 90$.

Figs. 4 and 5 show that covering the middle part of microbeam by a second layer with length of more than $0.7l$ dif not have a main effect on the static deflection and natural frequency; meaning that that this length was an optimized length and covering more than this length caused dissipation of the material.

Figures 6 to 9 show effect of electrostatic actuation on value of maximum static deflection and natural frequency of the microbeam. $h_2/h_1 = 0$ was assumed in Figs. 6 and 7 and $h_2/h_1 \neq 0$ in Figs. 8 and 9.

It was observed from these figures that, if $l_2 - l_1 \neq 0$, then with increasing value of $\alpha_2 v_p^2$, static deflection increased and natural frequency decreased. It must be noted that, in the plotted figures, the pull-in voltage was the voltage at which the system just lost its stability. So, it could be concluded from these figures that, with increasing value of $l_2 - l_1$, the pull-in voltage decreased. It was resulted from Figs. 6 and 8 that static deflection of the system under constant value of $\alpha_2 v_p^2$ increased by increasing value of $l_2 - l_1$.

Comparing Figs. 7 and 9 showed that, if value of $\alpha_2 v_p^2$ was assumed constant, then variations of natural frequency with increasing $l_2 - l_1$ in Fig. 7 were different from its variations in Fig. 8. Figure 7 demonstrates that, for all values of $\alpha_2 v_p^2$ by increasing value of $l_2 - l_1$, value of natural frequency decreased. But, Fig. 8 shows that, if value of $\alpha_2 v_p^2$ was far from the pull-in voltage, then natural frequency increased with increasing value of $l_2 - l_1$; and, if $\alpha_2 v_p^2$ was close to the pull-in voltage, then this behavior was reversed.

The reason is that, when $h_2/h_1 = 0$, then with increasing value of $l_2 - l_1$, bending stiffness remained constant. But, when $h_2/h_1 \neq 0$, then with increasing value of $l_2 - l_1$, the bending stiffness increased because the second layer would be deposited on the larger length of microbeam. When $\alpha_2 v_p^2$ was far from the pull-in voltage, the increase effect of equivalent bending stiffness was larger than increased softening electrostatic actuation. So, natural frequency increased with increasing value of $l_2 - l_1$, and with more increase of $\alpha_2 v_p^2$ and closeness to pull-in voltage, this competition would be reversed.

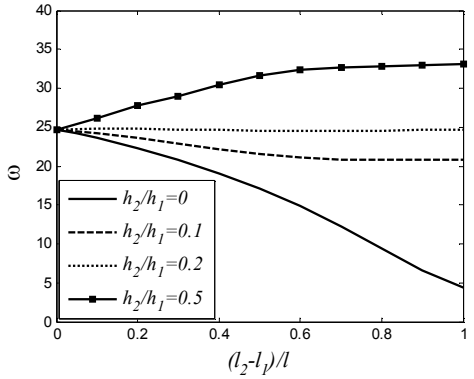

Fig. 5. The first natural frequency variations of the microbeam with respect to variation of $l_2 - l_1$ for different values of h_2/h_1, where $\alpha_2 v_p^2 = 90$.

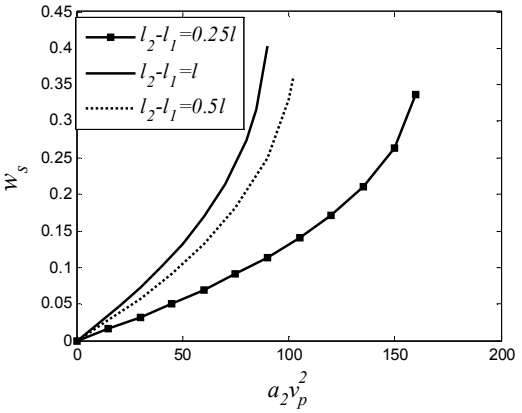

Fig. 6. Variations of the maximum deflection with respect to the variations of $\alpha_2 v_p^2$ for different values of $l_2 - l_1$, where $h_2 / h_1 = 0$.

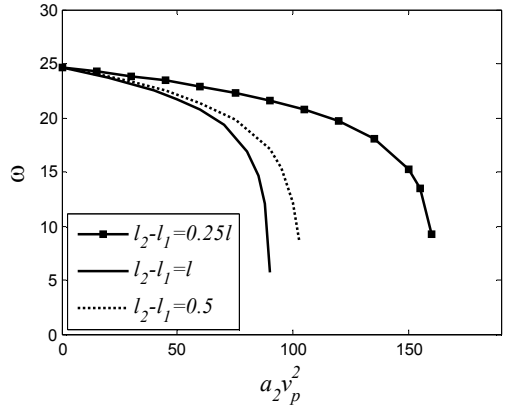

Fig. 7. Variations of the natural frequency with respect to the variations $\alpha_2 v_p^2$ for different values of $l_2 - l_1$, where $h_2 / h_1 = 0$.

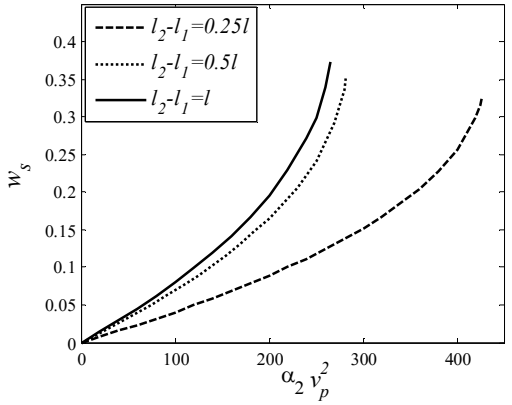

Fig. 8. Variations of the maximum deflection with respect to the variations of $\alpha_2 v_p^2$ for different values of $l_2 - l_1$, where $h_2 / h_1 = 0.5$.

Figure 10 shows variations of a_0 with respect to the variation of detuning parameter σ for different values of electrode plate length in the system with $h_2 / h_1 = 0$. It could be observed that, with increasing value of $(l_2 - l_1)/l$ from 0.2 to 0.4, hardening behavior of the system decreased, amplitude a_0 increased and nonlinear shift of resonance frequency decreased. Also, it was demonstrated that, with increasing value of $(l_2 - l_1)/l$ from 0.4 to 0.8, the system behaviorchanged to softening behavior. In addition, amplitude a_0 and nonlinear shift of resonance frequency increased.

The reason was that, considering Eq. (43), maximum value for a_0 was $2F/(\omega\mu)$ and nonlinear shift of resonance frequency was $4SF^2/(\omega^3\mu^2)$; in other words, if sign of S was positive (negative), then the system had a hardening (softening) behavior. In addition, it was demonstrated that value of amplitude and nonlinear shift of resonance frequency were altered due the competition between values of ω, S, μ and F. Considering Figs. 6 and 7, when $h_2 / h_1 = 0$, then with increasing value of $(l_2 - l_1)/l$, static deflection increased and natural frequency decreased. Considering Eqs. (36) and (40), value of F increased by increasing value of $l_2 - l_1$. These variations meant that maximum value of a_0 increased by increasing value of $l_2 - l_1$. Also, it was shown in Fig. 3 that value of S was positive or negative depending the competition between negative nonlinear electrostatic terms; i.e. S_c^E and S_q^E, and positive nonlinear geometric terms; i.e. S_c^G and S_q^G. Eqs. (36) and (40) demonstrate that absolute value of S_c^E and S_q^E increased by increasing value of $(l_2 - l_1)/l$ and w_s. With increasing value of $(l_2 - l_1)/l$ from 0.2 to 0.4, value of S decreased but remained positive. By more increase of $(l_2 - l_1)/l$, value of S changed to negative value;, so, the system behavior would be softening.

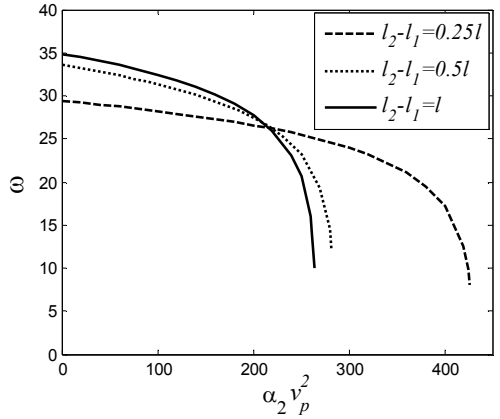

Fig. 9. Variations of the natural frequency with respect to variations of $\alpha_2 v_p^2$ for different values of $l_2 - l_1$ where $h_2 / h_1 = 0.5$.

Figure 11 shows that, in contrast to to Fig. 10, the hardening behavior did not change to softening behavior by increasing value of $(l_2 - l_1)/l$. The reason of this difference could be that, considering Figs. 4 and 5, when $h_2 / h_1 \neq 0$, then increase of w_s by increasing value of $(l_2 - l_1)/l$ was smaller than its increase when $h_2 / h_1 = 0$. In other words, absolute value of softening electrostatic terms; i.e. S_c^E and S_q^E; had low increase; so, value of S did not change to a negative value. It means that behavior of the system remained as hardening by increasing value of $(l_2 - l_1)/l$.

Figure 12 shows variations of a_0 with respect to variations of detuning parameter σ for different values of the second layer thickness. It was demonstrated that, for $h_2 / h_1 = 0$, the system had a softening behavior. It is concluded that, by increasing value of h_2 / h_1 from 0 to 0.25, the system behavior changed to hardening. Also, it was resulted that, by increasing value of h_2 / h_1 from 0.25 to 0.5, amplitude a_0 and nonlinear shift of resonance frequency decreased. These variations were due to the fact that, considering the above discussion, if $h_2 / h_1 = 0$, then value of the static deflection would be large.

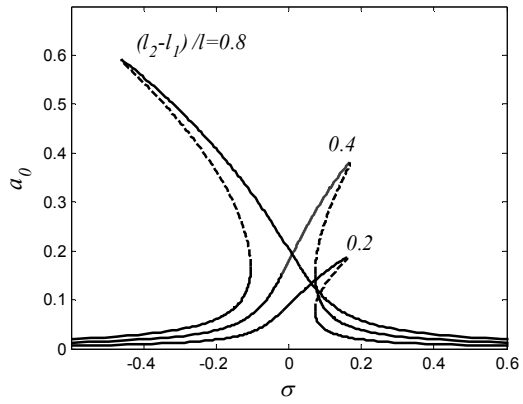

Fig. 10. Variations of a_0 with respect to the variations of σ for different values of $(l_2 - l_1)/l$ where $h_2 / h_1 = 0$, $\alpha_2 v_p^2 = 45$, $v_{ac} = 0.02$. Solid lines belong to stable solution, and dashed lines belong to unstable solution.

It has been mentioned that, in this condition, value of S would be negative. In other words, the system had a softening behavior. With increasing the value of h_2 / h_1, static deflection decreased; so, value of S changed to a positive value. Also, value of ω increased. Therefore, considering Eq. (43), value of a_0 decreased.

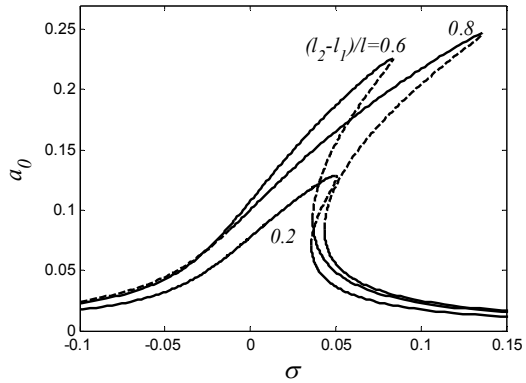

Fig. 11. Variations of a_0 with respect to the variations of σ for different values of $(l_2 - l_1)/l$ where $h_2 / h_1 = 1$, $\alpha_2 v_p^2 = 45$, $v_{ac} = 0.02$. Solid lines belong to stable solution, and dashed lines belong to unstable solution.

It must be noted that the nonlinear shift of resonance frequency due to the stretching effect was a disadvantage in the design of microresonator system. This nonlinear shift was

removed by the softening effect of electrostatic actuation. It is shown in Fig. 10 that, with selecting a proper length for electrostatic actuation, the nonlinear shift might be removed. It is noted that, in this configuration (partially actuated), the consumption of electric energy was lower than the case including electrostatic actuation at the entire length, which was a good advantage.

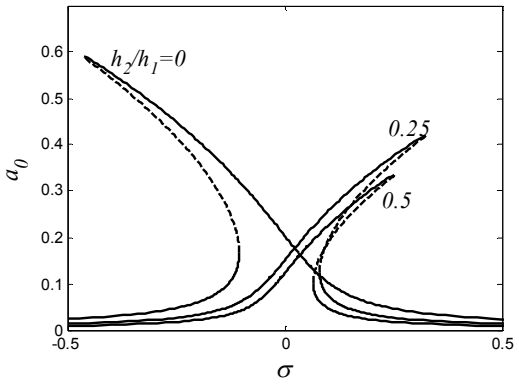

Fig. 12. Variations of a_0 with respect to the variations of σ for different values of h_2/h_1 where $l_2 - l_1 = 0.8l$, $\alpha_2 v_p^2 = 45$, $v_{ac} = 0.02$. Solid lines belong to stable solution, and dashed lines belong to unstable solution.

6. Conclusions

In this paper, static deflection, natural frequency and nonlinear vibration of a clamped-clamped two layered microbeam under discontinuous electrostatic actuation were studied. It was shown that, depending on the value of electrode plate length, the second layer thickness and value of electrostatic actuation, a softening or hardening behavior might be realized. It was observed that, with increasing the value of electrode plate length, value of static deflection increased and pull-in voltage decreased. In addition, it was resulted that, for small value of h_2/h_1, by increasing value of electrode plate length, value of natural frequency decreased and, for a larger value of h_2/h_1, this behavior was reversed. Moreover, by increasing value of electrostatic actuation, the static deflection increased and natural frequency decreased. Also, it could be concluded that, when the system did not have the second layer, then for all values of $\alpha_2 v_p^2$, natural frequency increased by increasing value of $l_2 - l_1$. Furthermore, when there was the second layer on the lower side of microbeam, then for small value of $\alpha_2 v_p^2$, natural frequency increased by increasing the value of $l_2 - l_1$ and a more increase in the value of $\alpha_2 v_p^2$ reversed this behavior.

The results demonstrated that, when $h_2/h_1 = 0$ and the system had an initially hardening behavior, then by increasing the value of $l_2 - l_1$, amplitude and linear behavior increased and, by a more increase in the values of $l_2 - l_1$, it might be changed to the softening behavior. It was also shown that a different behavior was observed when the value of h_2/h_1 was large.

Accordingly, when the system had an initially softening behavior, then, by increasing value of h_2/h_1, linear behavior increased. In addition, amplitude a_0 decreased and, by a more increase in the value of h_2/h_1, its behavior changed to a hardening behavior and amplitude had a more decrease.

Acknowledgment

The study was performed in School of Engineering, Kharazmi University, under a grant presented by Vice Chancellor in Research, which should be acknowledged.

References:

[1] M. I. Younis and A. H. Nayfeh, "A Study of the nonlinear response of a resonant microbeam to an electric actuation", *Nonlinear Dyn.,*Vol. 31, No. 1, pp. 91-117,(2003).

[2] H. A. Tilmans and R. Legtenberg, "Electrostatically driven vacuum-encapsulated polysilicon resonator part ii: Theory and performance", *Sensors Actuators A*, Vol. 45, No. 1, pp. 67-84, (1994) .

[3] B. Choi and E. G. Lovell, "Improved analysis of microbeams under mechanical and electrostatic loads", *J. Micromech. Microeng.*, Vol. 7, No. 1, pp. 24-29, (1997).

[4] E. M. Abdel-Rahman, M. I. Younis and A. H. Nayfeh, "Characterization of the mechanical behavior of an electrically actuated microbeam", *J. Micromech. Microeng.*, Vol. 12, No. 6, pp. 759-766, (2002).

[5] M. I. Younis, E. M. Abdel-Rahman and A H Nayfeh, "A reduced-order model for electrically actuated microbeam–based MEMS", *J. Microelectromech. Syst.* , Vol. 12, No. 5, pp. 672-680, (2003).

[6] S. Chaterjee and G. Pohit, "A large deflection model for the pull-in analysis of electrostatically actuated microcantilever beams", *J. Sound. Vib.*, Vol. 322, No. 4, pp. 969-986, (2009).

[7] M. Rasekh and S. E. Khadem, "Pull-in analysis of an electrostatically actuated nano-cantilever beam with nonlinearity in curvature and inertia", *Int. J. Mech. Sci.*, Vol. 53, No. 2, pp. 108-115, (2011).

[8] X. Lizhong and J. Xiaoli, "Electromechanical coupled nonlinear dynamics for microbeams", *Arch. Appl. Mech.*, Vol. 77, No. 7, pp. 485-502, (2007).

[9] D. I. Caruntu and M. Knecht, "On nonlinear response near-half natural frequency of electrostatically actuated microresonator", *Int. J. Str. Stab. Dyn.*, Vol. 11, No. 4, pp. 641-672, (2011).

[10] P. Kim, S. Bae and J. Seok, "Resonant behaviors of a nonlinear cantilever beam with tip mass subject to an axial force and electrostatic excitation", *Int. J. Mech. Sci.*, Vol. 64, No. 1, pp. 232-257, (2012).

[11] E. M. Abdel-Rahman and A. H. Nayfeh, "Secondary resonances of electrically actuated resonant microsensors", *J. Micromech. Microeng,* Vol. 13, No. 1, pp. 491-501, (2003).

[12] X. L. Jia, J. Yang, S. Kitipornchai and C.W. Lim, "Resonance frequency response of geometrically nonlinear micro-switches under electrical actuation", *J. Sound. Vib.*, Vol. 331, No. 14, pp. 3397-3411, (2012).

[13] F. Najar, S. Choura, S. E. Borgi, E. M. Abdel-Rahman and A. H. Nayfeh, "Modeling and design of variable-geometry electrostatic microactuators", *J. Micromech. Microeng.,* Vol. 15, No. 3, pp. 419-429, (2005).

[14] M. Abdalla, C. K. Reddy, W. Faris and Z. Gurdal, "Optimal design of an electrostatically actuated microbeam for maximum pull-in voltage", *Comput. Struct.,* Vol. 83, No. 15, pp. 1320-1329, (2005).

[15] M. Nie, Q. Huang and W. Li, "Measurement of material properties of individual layers for composite films by a pull-in method", *J. Phys.: Conf. Series.*, Vol. 34, No. 1, pp. 516-521, (2006).

[16] G. Rezazadeh, "A comprehensive model to study nonlinear behavior of multilayered micro beam switches", *Microsyst.Technol.*, Vol. 14, No. 1, pp. 135-141, (2007).

[17] Y. G. Wang, W. H. Lin, Z. J. Feng and X. M. Li, "Characterization of extensional multi-layer microbeams in pull-in phenomenon and vibrations", *Int. J. Mech. Sci.*, Vol. 54, No. 1, pp. 225-233, (2012).

[18] X. L. Jia, J. Yang, S. Kitipornchai and C. W. Lim, "Pull-in instability and free vibration of electrically actuated poly-SiGe graded micro-beams with a curved ground electrode", *Appl. Math. Modell.*, Vol. 36, No. 5, pp. 1875-1884, (2012).

[19] H. Sadeghian, G. Rezazadeh, E. Malekpour and A. Shafipour, "Pull-In voltage of fixed-fixed end type MEMS switches with variative electrostatic area", *sensor and transducer.*, Vol. 66, No. 4, pp. 526-533, (2006).

[20] M. I. Younis, *MEMS linear and nonlinear statics and dynamics*, Springer, New York, pp. 312-315, (2011).

[21] A. Fargas, R. Costa and A. M. Shkel, "Modeling the Electrostatic Actuation of MEMS: State of The Art 2005", Institut d'Organitzaci o i Control de Sistemes

Industrials, IOC-UPC and University of California at Irvine, (2005).

[22] A. H. Nayfeh and P. F. Pai, *Linear and nonlinear structural mechanics*, John Wiley & Sons, New York, pp. 220-221, (2004).

[23] M, Zamanian and S. E. Khadem, "Nonlinear vibration of an electrically actuated microresonator tuned by combined DC piezoelectric and electric", *Smart Mater. Struct.*, Vol. 19, No. 1, 015012, (2010).